



Synthesis and photophysical studies of a multivalent photoreactive Ru^{II}-calix[4]arene complex bearing RGD-containing cyclopentapeptides

Sofia Kajouj¹, Lionel Marcelis^{*1,2}, Alice Mattiuzzi³, Adrien Grassin⁴, Damien Dufour⁵, Pierre Van Antwerpen⁵, Didier Boturyn⁴, Eric Defrancq⁴, Mathieu Surin⁶, Julien De Winter⁷, Pascal Gerbaux⁷, Ivan Jabin^{*3} and Cécile Moucheron^{*1}

Full Research Paper

[Open Access](#)

Address:

¹Laboratoire de Chimie Organique et Photochimie, Université libre de Bruxelles, Avenue F.D. Roosevelt 50, CP 160/08, 1050 Bruxelles, Belgium, ²Engineering of Molecular NanoSystems, Ecole Polytechnique de Bruxelles, Université libre de Bruxelles (ULB), Avenue F.D. Roosevelt 50, CP165/64, B-1050 Brussels, Belgium, ³Laboratoire de Chimie Organique, Université libre de Bruxelles, Avenue F.D. Roosevelt 50, CP 160/06, 1050 Bruxelles, Belgium, ⁴Université Grenoble Alpes, Département de Chimie Moléculaire UMR CNRS 5250, CS 40700, 38058 Grenoble Cedex 09, France, ⁵Analytical Platform of the Faculty of Pharmacy, Université libre de Bruxelles, Boulevard du Triomphe, Campus de la Plaine, CP205/05, 1050 Bruxelles, Belgium, ⁶Laboratory for Chemistry of Novel Materials, Center for Innovation and Research in Materials and Polymers, University of Mons – UMONS, 20, Place du Parc, B-7000 Mons, Belgium and ⁷Organic synthesis and Mass Spectrometry Laboratory, University of Mons - UMONS, Place du Parc 23, B-7000 Mons, Belgium

Email:

Lionel Marcelis^{*} - lmarceli@ulb.ac.be; Ivan Jabin^{*} - ijabin@ulb.ac.be; Cécile Moucheron^{*} - cmouche@ulb.ac.be

^{*} Corresponding author

Keywords:

anticancer drug; calixarene; cell targeting; RGD peptide; ruthenium complex

Beilstein J. Org. Chem. **2018**, *14*, 1758–1768.

doi:10.3762/bjoc.14.150

Received: 15 April 2018

Accepted: 21 June 2018

Published: 16 July 2018

This article is part of the thematic issue "Macrocyclic and supramolecular chemistry".

Guest Editor: M.-X. Wang

© 2018 Kajouj et al.; licensee Beilstein-Institut.

License and terms: see end of document.

Abstract

Photoactive ruthenium-based complexes are actively studied for their biological applications as potential theragnostic agents against cancer. One major issue of these inorganic complexes is to penetrate inside cells in order to fulfil their function, either sensing the internal cell environment or exert a photocytotoxic activity. The use of lipophilic ligands allows the corresponding ruthenium complexes to passively diffuse inside cells but limits their structural and photophysical properties. Moreover, this strategy does not provide any cell selectivity. This limitation is also faced by complexes anchored on cell-penetrating peptides. In order to provide a selective cell targeting, we developed a multivalent system composed of a photoreactive ruthenium(II) complex tethered to a

calix[4]arene platform bearing multiple RGD-containing cyclopentapeptides. Extensive photophysical and photochemical characterizations of this Ru(II)–calixarene conjugate as well as the study of its photoreactivity in the presence of guanosine monophosphate have been achieved. The results show that the ruthenium complex should be able to perform efficiently its photoinduced cytotoxic activity, once incorporated into targeted cancer cells thanks to the multivalent platform.

Introduction

Long-living luminescent polyazaaromatic ruthenium(II) complexes are intensively studied in a biological context, in particular (i) for their ability to sense their environment and (ii) for their photoreactivity towards relevant biological targets [1–4]. Sensors for biological species are mostly based on complexes bearing the well-known dppz ligand (dppz = dipyrido[3,2-*a*:2',3'-*c*]phenazine) and its derivatives. J. K. Barton et al. demonstrated in 1990 that $[\text{Ru}(\text{bpy})_2(\text{dppz})]^{2+}$ behaves as a light-switch for DNA [5]: this complex is not luminescent in water but upon intercalation within the DNA base pairs stack, the complex luminescence is restored. Derivatives of $[\text{Ru}(\text{bpy})_2(\text{dppz})]^{2+}$ and complexes bearing similar aromatic planar ligands were developed to probe specific sites of DNA, such as mismatches [6–8], abasic sites [9] or G-quadruplexes [10,11]. Aside photosensors, photoreactive complexes able to damage biological targets were also developed. These complexes are mainly used to induce damages in cancerous cells upon light irradiation. Two types of photooxidative damages can be induced: (i) by photosensitization of singlet oxygen and subsequent generation of highly reactive oxygen species (ROS) (type I photosensitization) or (ii) by direct oxidative electron transfer to biological molecules such as DNA or amino acids (type II photosensitization). In particular, it was shown that Ru^{II} complexes containing at least two highly π -deficient polyazaaromatic ligands such as 1,4,5,8-tetraazaphenanthrene (TAP) [12–14] or 1,4,5,8,9,12-hexaazatriphenylene (HAT) [15] are able to oxidize the guanine base (G) of DNA or the tryptophan (Trp) amino acid residue through a photoinduced electron-transfer (PET) process [16–19]. Interestingly, the two radical species generated by this PET can recombine to form a covalent photoadduct [20–22]. When this photoadduct is formed with the guanine base, the activity of enzymes such as RNA polymerase or endonuclease is inhibited in vitro at the level of the photoadduct [23,24]. In order to target a specific DNA sequence, photoreactive Ru^{II} complexes have been anchored to specific antisense oligonucleotides to inhibit the expression of the complementary targeted genes under illumination [25,26]. This photoinduced gene-silencing strategy has been proven to be also efficient in living cells [27,28], paving the way for the use of photoactivable Ru^{II} complexes as photocontrolled anti-cancer therapeutic agents.

Despite their interesting photochemical properties, photoreactive Ru^{II} complexes have shown low cell-penetration efficiency,

preventing their direct use in biological applications. More lipophilic ligands such as bathophenanthroline and modified dppz were developed and the internalization of the corresponding Ru^{II} complexes was demonstrated [29–32]. These complexes are however not photoreactive due to the absence of π -deficient ligands. More recently, Ru^{II} complexes bearing two modified TAP ligands with highly lipophilic moieties were reported [33]. These compounds are able to enter the cells and photoinduce caspase-dependent and reactive-oxygen-species-dependent apoptosis. Another strategy for the design of cell penetrating photoreactive Ru^{II} complexes consists of tethering the complex to a vector that allows a cellular uptake. In this context, Os^{II}, Rh^{III} and Ru^{II} complexes were anchored to cell penetrating peptides (CPP) such as polyarginine [34–37]. The tethering of a photoreactive Ru^{II} complex on the *transactivating transcriptional activator* (TAT) peptide was also reported and it was shown that the corresponding Ru^{II} conjugate could be internalized inside HeLa cells without any modification of the photochemical properties of the complex [38].

It should be noted that modifications of ligands to make the resulting complexes more lipophilic or the conjugation of a complex to a CPP do not provide any control on the way these complexes will be internalized by cells and prevent thus any targeting of malignant cells over healthy ones. The next step in the development of phototherapeutic agents based on polyazaaromatic Ru^{II} complexes is thus the specific targeting of cancerous cells. In this regard, $\alpha_v\beta_3$ integrin represents an interesting target as this membrane receptor is overexpressed in the endothelial cells of neoangiogenic vessels and in several human tumor cells [39,40]. It is well known that RGD-containing oligopeptides (RGD = Arg-Gly-Asp tripeptide pattern) bind selectively to $\alpha_v\beta_3$ integrin with a high affinity and a very high selectivity [41–43]. As multivalency enhances the binding strength of a ligand to its receptor [44–46], clustered RGD-containing compounds were developed and were shown to exhibit attractive biological properties for the imaging of tumors [47–50] and for the targeted drug delivery [51–53].

In the course of designing phototherapeutic agents that could specifically target cancerous cells, we envisaged to graft a photoreactive Ru^{II} complex on a multivalent platform decorated with multiple RGD-containing cyclopentapeptides. A calix[4]arene moiety was chosen as the multivalent platform as

this rigid macrocycle displays two distinct faces that can be selectively functionalized [54–56]. It is noteworthy that the calix[4]arene skeleton has been already exploited for the development of multivalent glyco- and peptidocalixarenes that can be recognized by cell-membrane receptors [57–59] and of calixarene derivatives able to specifically target membrane proteins involved in the angiogenesis process [60]. Furthermore, the use of calixarenes for biological applications is the subject of intensive researches. They are indeed exploited in various areas such as surface recognition, structural mimics or membrane receptor inhibition [61–63], and it was also shown that calixarenes themselves display antibacterial, antiviral, and anti-cancer properties [64].

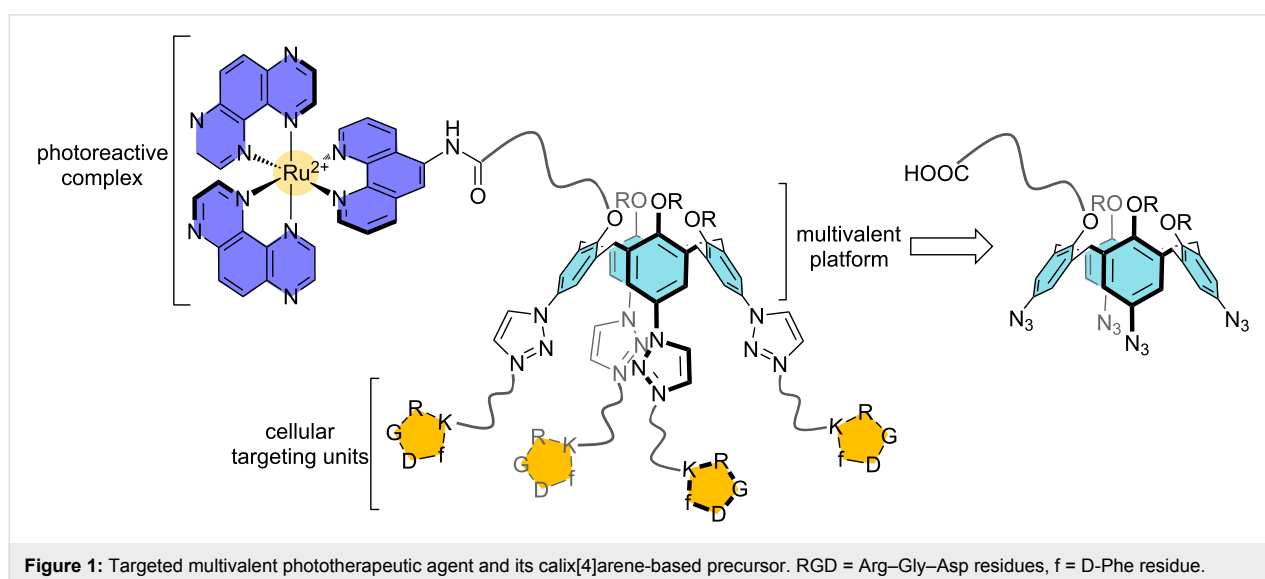
Herein, we describe the synthesis of a multivalent phototherapeutic agent designed in order to specifically target membrane receptors involved in the angiogenesis process. The multivalent system is composed of a photoreactive $[\text{Ru}(\text{TAP})_2\text{phen}]^{2+}$ complex tethered to a calix[4]arene platform bearing four *c*-[RGDfK] moieties [65] (Figure 1). Before studying this conjugate in vitro, it was first mandatory to check that the photochemistry of the Ru^{II} complex was not altered by the presence of the targeting platform. The photophysical properties of this Ru^{II} –calixarene conjugate were thus examined and compared to those of the reference complex $[\text{Ru}(\text{TAP})_2\text{phen}]^{2+}$.

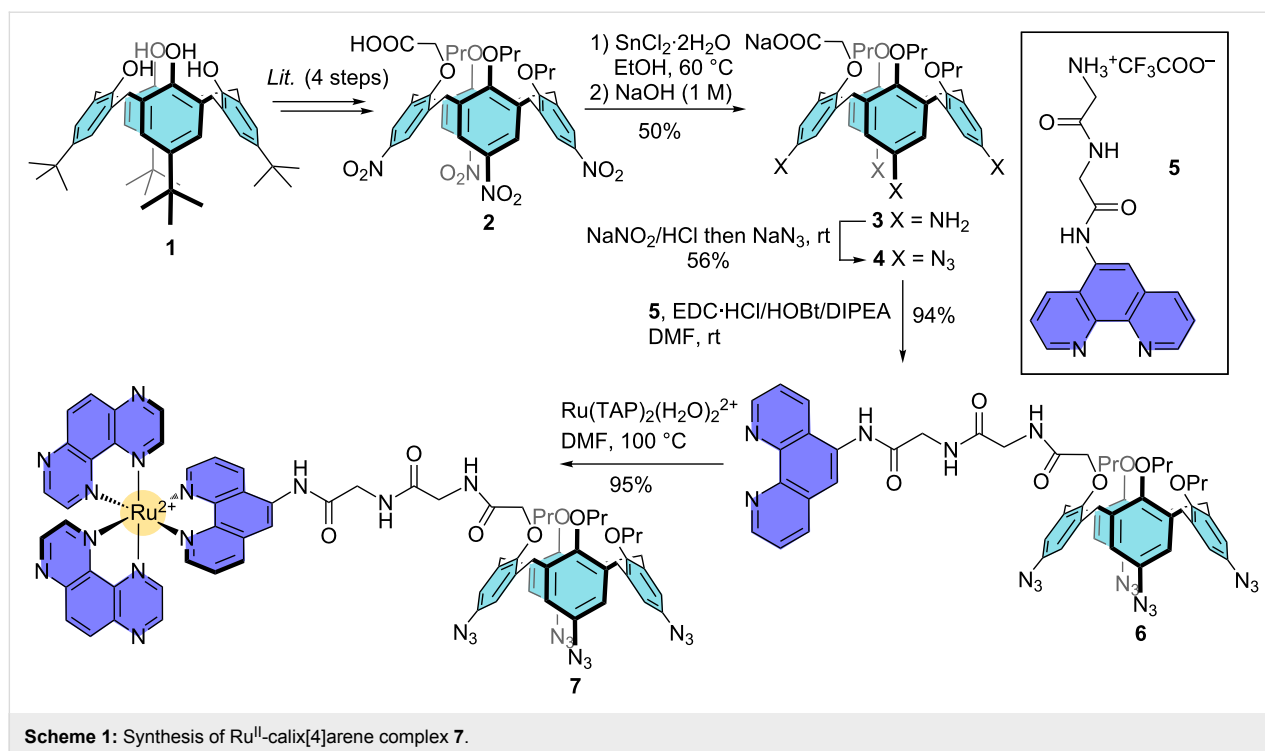
Results and Discussion

Synthesis of Ru^{II} –calixarene conjugate **9**

For the synthesis of the target multivalent system, the strategy relies on the anchoring i) of the photoreactive $[\text{Ru}(\text{TAP})_2\text{phen}]^{2+}$ complex on the calix[4]arene small rim through a peptide-type coupling and ii) of the four *c*-[RGDfK] moieties on the opposite rim through a copper-catalyzed

azide–alkyne cycloaddition (CuAAC) [66–68] (Figure 1). It was thus necessary to block the calix[4]arene skeleton in the cone conformation and to functionalize separately the two distinct rims (Scheme 1). Firstly, known calixarene **2** with an appending carboxylate arm on the small rim was synthesized from commercial *p*-*tert*-butylcalix[4]arene **1** according to a four-step sequence [69]. Note that propyl groups were chosen for the modification of the small rim because these groups are the smallest possible for blocking the oxygen-through-the-annulus rotation of the aromatic units [70]. The nitro groups of **2** were then reduced using $\text{SnCl}_2 \cdot 2\text{H}_2\text{O}$ in ethanol, affording tetra-amino compound **3** [69] in 50% yield. Diazotation followed by nucleophilic substitution with sodium azide gave the desired tetra-azido compound **4** in 56% overall yield from **3**. It is noteworthy that the introduction of the azido groups on the calix[4]arene scaffold was clearly confirmed by the presence of an intense band at 2108 cm^{-1} in the IR spectrum of **4**. Phenanthroline derivative **5** was synthesized from 5-glycinamido-1,10-phenanthroline in a two-step sequence consisting of a peptide-type coupling reaction with a Boc-protected glycine *N*-hydro-succinimide ester followed by the deprotection of the amino group (see Supporting Information File 1) [71]. Different coupling agents (DCC/HOBt, EDC-HCl/HOBt, PyBOP) and conditions were then tested for the peptide-type coupling reaction between calix[4]arene **4** and phenanthroline derivative **5**. The use of an excess of **5** (2 equiv) in the presence of EDC-HCl and HOBt in DMF at room temperature led to the best yield and the easiest purification process. Under these optimal conditions, the desired compound **6** was isolated in a high 94% yield. Finally, the reaction between $[\text{Ru}(\text{TAP})_2(\text{H}_2\text{O})_2]^{2+}$ and **6** in DMF at $100\text{ }^\circ\text{C}$ gave the Ru^{II} –calix[4]arene complex **7** in 95% yield after C18 reversed-phase silica gel column chromatographic purification. Complex **7** was fully characterized by 1D and



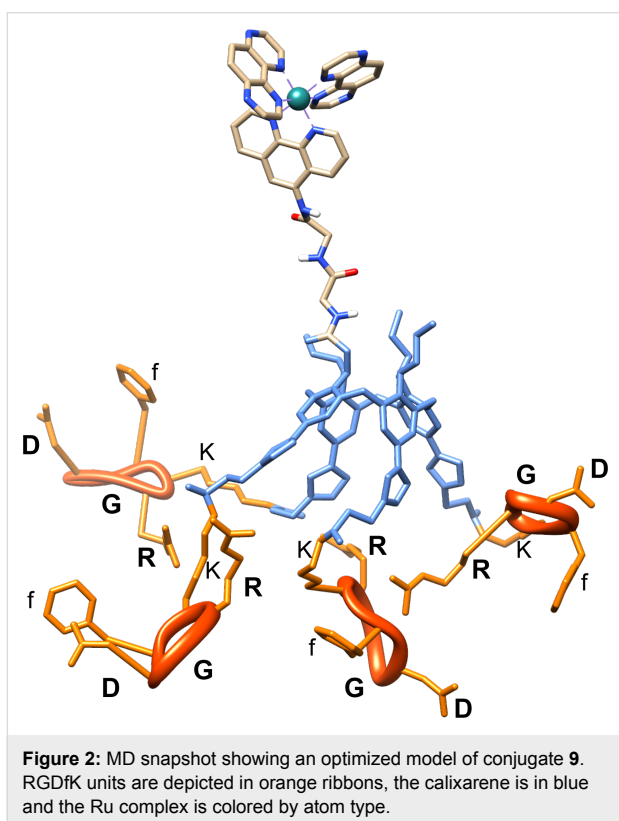
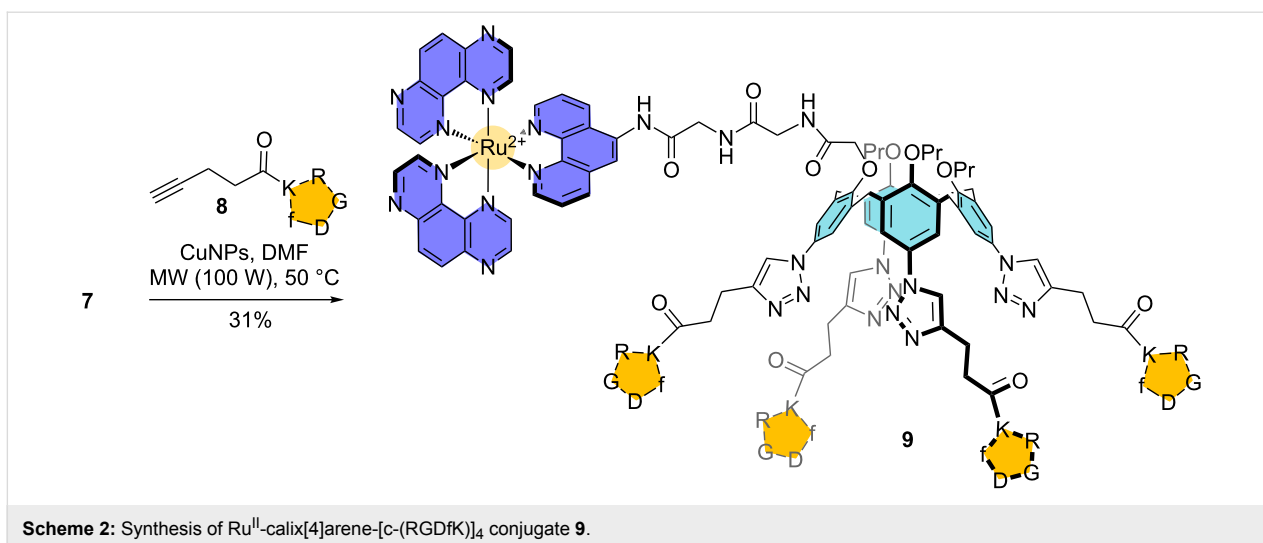


2D NMR spectroscopy in CD₃CN at 600 MHz. In accordance with the presence for the chiral Ru(TAP)₂phen moiety, the ¹H NMR spectrum of **7** is characteristic of a C₁ symmetrical compound as all the protons belonging to the ArH, ArCH₂ and OPr group are differentiated. Moreover, complex **7** was also characterized by high-resolution mass spectrometry (HRMS). The ESI mass spectrum displays two intense signals at *m/z* 764.736 and *m/z* 1642.456 that are attributed respectively to the doubly charged **7**²⁺ and singly charged [**7** + CF₃COO⁻]⁺ by comparison between the experimental and theoretical isotope distributions (see Supporting Information File 1).

With Ru^{II}-calix[4]arene complex **7** in hands, we next moved to the introduction of the cellular targeting units on the large rim through copper-catalyzed azide–alkyne cycloaddition (CuAAC). Note that the triazole moieties that would result from such a cycloaddition are known to be stable towards hydrolysis and protease, which allows their use in a biological environment [72]. For the CuAAC, the use of Cu^I-generated in situ from a mixture of CuSO₄·5H₂O and sodium ascorbate is often reported in the field of calixarene chemistry [66,73–78]. Unfortunately, this methodology led to poor yields and a lack of reproducibility in the case of calixarene **7** and c-[RGDfK]-alkyne **8**, even when a microwave heating was used. We then evaluated the use of copper nanoparticles (CuNPs), as these nanomaterials are known to catalyze efficiently a wide range of organic reactions and notably the azide–alkyne cycloaddition [79]. Calixarene **7** was reacted with a slight excess (5 equiv) of

cyclopeptide **8** in the presence of CuNPs and the mixture was heated by microwave (100 W) at 50 °C for 1 hour. The use of CuNPs greatly facilitated the monitoring of the reaction and the work-up, as these nanomaterials being easily removed from the crude mixture by simple centrifugation. To our delight, [Ru(TAP)₂phen]²⁺-calix[4]arene-[c-(RGDfK)]₄ conjugate **9** was isolated in 31% yield after purification by semi-preparative RP-HPLC (Scheme 2). The successful synthesis and purification of conjugate **9** was also confirmed by HRMS. Indeed, the ESI mass spectrum features several peaks corresponding to characteristic ions of different charge states at *m/z* 1421.577 (3+), 1066.434 (4+) and 853.556 (5+) that are attributed to [**9** + H]³⁺, [**9** + 2H]⁴⁺ and [**9** + 3H]⁵⁺ by comparison between the experimental and theoretical isotope distributions (see Supporting Information File 1).

Molecular modeling simulations were carried out to provide insights into the size and morphology of conjugate **9**. An optimized geometry is presented in Figure 2, as issued from a molecular dynamics (MD) simulations. The ruthenium complex and the RGD units are spatially well-separated thanks to their grafting on opposite faces of the rigid calixarene-based platform. In this conformation, the distances between the Ru atom and each of the nearest carbon atoms of RGDfK units exceed 30 Å. Along the MD simulations, we noticed that the Ru complex remained far from the cyclic pentapeptides. This is due to the fact that the linkers of each arm are smaller than the size of the calixarene platform, preventing contacts between the Ru



complex and the RGDfK units. The global structure has an average radius of gyration R_g of $1.25 \text{ nm} \pm 0.1 \text{ nm}$. Noteworthy, the distance between the RGDfK units largely varies along the MD simulations, ranging from 10 \AA to 24 \AA (average at 17 \AA), as estimated from the distance between equivalent carbon atoms crossing the linker and the cyclic pentapeptides. This large variation in the distance is due to the flexibility of the linkers between the calixarene platform and the RGDfK units, together with the many possibilities of H-bonding between: (i) oxygen

atoms at C=O in the linker and the hydrogen atoms of (N–H) of arginine of a neighboring ‘arm’; (ii) H-bonds between arginine terminal N–H and C=O of the peptide bond of phenylalanine of an adjacent cyclic pentapeptide (see Supporting Information File 1), yielding adjacent cyclic pentapeptides in close proximity for a large set of conformations.

This separation between the Ru complex and the cyclic peptides by the calixarene should be an advantage by preventing any negative effect of the RGD peptidic units on the photochemistry of the complex and, alternatively, prevents any influence of the complex on the affinity of the RGD patterns to interact with the targeted integrins. However, the possible H-bonding interactions between neighboring RGD units could be a drawback in view of the accessibility of the arginine groups to interact with the integrins.

Photophysical properties of Ru^{II}-calixarene conjugate **9**

The absorption and emission spectra of Ru-calix(RGD)₄ conjugate **9** (as its CF_3COO^- salt) were recorded in water at room temperature (Figure 3). These spectroscopic data are gathered in Table 1 with the ones of the free $[\text{Ru}(\text{TAP})_2\text{phen}]^{2+}$ complex for comparison purpose.

Conjugate **9** exhibits absorption bands at 416 and 458 nm that corresponds to $d\pi(\text{Ru})-\pi^*(\text{phen}/\text{TAP})$ metal-to-ligand charge transitions (MLCT) similarly to what is observed for the untethered $[\text{Ru}(\text{TAP})_2\text{phen}]^{2+}$ complex (MLCT bands at 412 and 464 nm). The presence of the calix[4]arene platform has thus no impact on the visible part of the spectrum. The influence of the calixarene moiety is however visible in the UV region of the spectrum (around 200 nm) where the absorption bands are more intense. This increase is due to the contribution of the peptidic

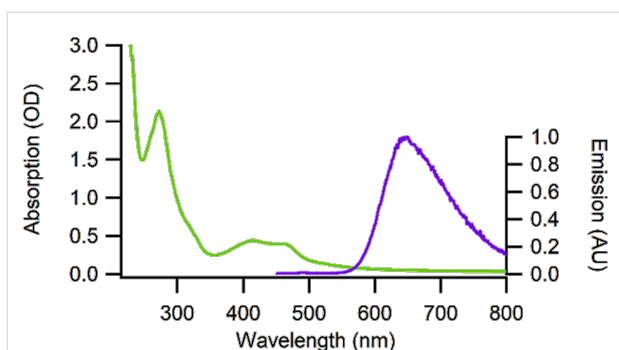


Figure 3: Absorption and emission spectra of Ru^{II}-calix[4]arene-[c-(RGDFK)₄] conjugate **9** in water.

subunits of the RGD moieties and of the aromatic units of the calixarene. It should be noted that the absorption at wavelengths longer than 550 nm does not go perfectly down to zero. This phenomenon is likely due to some light scattering caused by the presence of some small aggregates in solution. It appears that conjugate **9** is not completely soluble in pure water despite the presence of the charged Ru^{II} complex and the peptidic moieties on the calix[4]arene scaffold. Fortunately, these small aggregates totally disappeared when only 5% of DMSO was added to the medium [80].

The photoluminescence emission originating from the ³MLCT state is centered at 645 nm for both conjugate **9** and reference [Ru(TAP)₂phen]²⁺ complex. We measured the luminescence lifetime and determined the quantum yield of luminescence under air and argon atmosphere for conjugate **9** and reference [Ru(TAP)₂phen]²⁺ in water with 5% DMSO in order to avoid any formation of aggregates. The data gathered in Table 1 clearly indicate that the tethering of the [Ru(TAP)₂phen]²⁺ complex onto the calixarene platform does not induce any modification of the photophysical properties of the complex. In order to rule out any intramolecular quenching processes, control experiments were realized with the complex grafted onto the unmodified calixarene (conjugate **7**) in the presence of free cyclic pentapeptide units c-[RGDFK] **8** (see Supporting Information File 1). No modification of the luminescence by intermolecular quenching was observed, confirming the absence of internal quenching in the conjugate **9**.

Photoreactivity of Ru^{II}-calixarene conjugate **9**

The photoreactivity of Ru-TAP complexes is based on their ability to induce direct oxidation of guanine upon light excitation. In order to confirm that the tethering onto the calixarene platform does not impede the conjugated complex to photoreact with its biological target, we measured the evolution of the luminescence intensity and the excited state lifetime of conjugate **9** as function of the concentration of guanosine monophosphate (GMP, Figure 4).

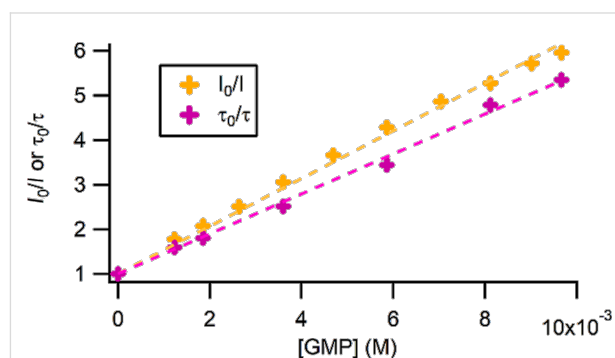


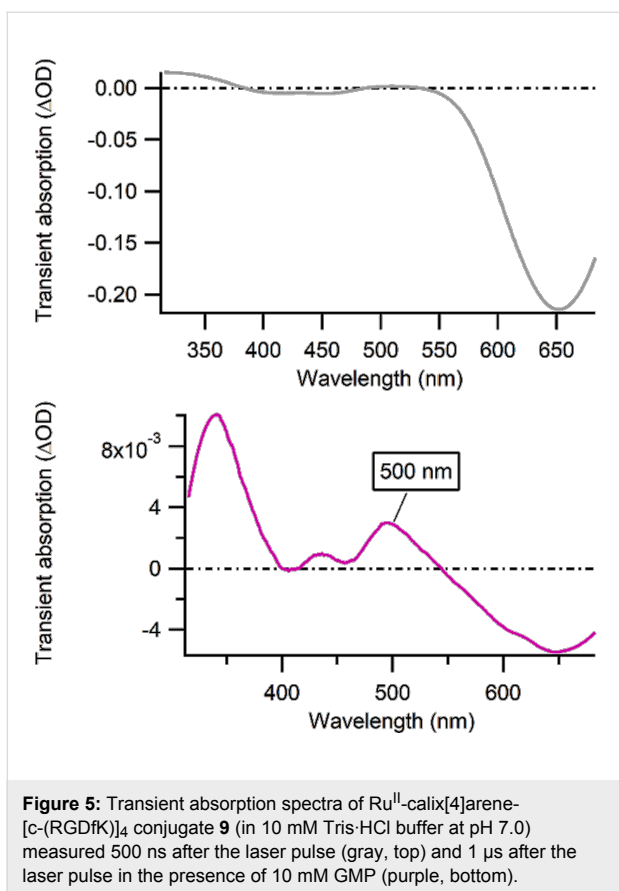
Figure 4: Luminescence intensity and excited state lifetime of conjugate **9** in the presence of GMP measured in 10 mM Tris-HCl buffer at pH 7.0.

Stern–Volmer analyses indicate that a dynamic quenching is occurring, with a quenching rate close to the diffusion limit ($k_Q = 5.6 \cdot 10^8 \text{ M}^{-1}\text{s}^{-1}$ in intensity and $k_Q = 5.3 \cdot 10^8 \text{ M}^{-1}\text{s}^{-1}$ in lifetime). This quenching of the luminescence of conjugate **9** in the presence of GMP reveals that a photoinduced electron transfer can take place between the excited complex and the guanine moiety, which could give rise to the formation of a photoadduct from the recombination of the monoreduced complex and the radical guanine generated after the photoinduced electron transfer (PET). In order to confirm the occurrence of PET, transient absorption measurements with conjugate **9** were performed in the absence and in the presence of GMP. The recorded transient absorption spectra are presented in Figure 5. In absence of GMP, the transient absorption spectrum of conjugate **9** is dominated by the luminescence, the ground state bleaching and some excited state absorption around 340 nm whereas in the presence of GMP a positive transient signal can

Table 1: Photophysical properties of conjugate **9** and [Ru(TAP)₂phen]²⁺ in water.

Complex	λ^{abs} (nm)	λ^{em} (nm)	$\Phi^{\text{Air a,b}}$	$\Phi^{\text{Ar a,b}}$	$\tau_{\text{av}}^{\text{Air b,c}}$ (ns)	$\tau_{\text{av}}^{\text{Ar b,c}}$ (ns)
[Ru(TAP) ₂ phen] ²⁺	231, 272, 412, 464	645	0.029	0.055	714	891
conjugate 9	274, 416, 458	645	0.025	0.044	901	1087

^aPhotoluminescence quantum yields are determined by comparison with [Ru(bpy)₃]²⁺. Errors on Φ estimated to <20%. ^bMeasurement with 5% DMSO. ^cErrors on lifetime estimated to 15%.

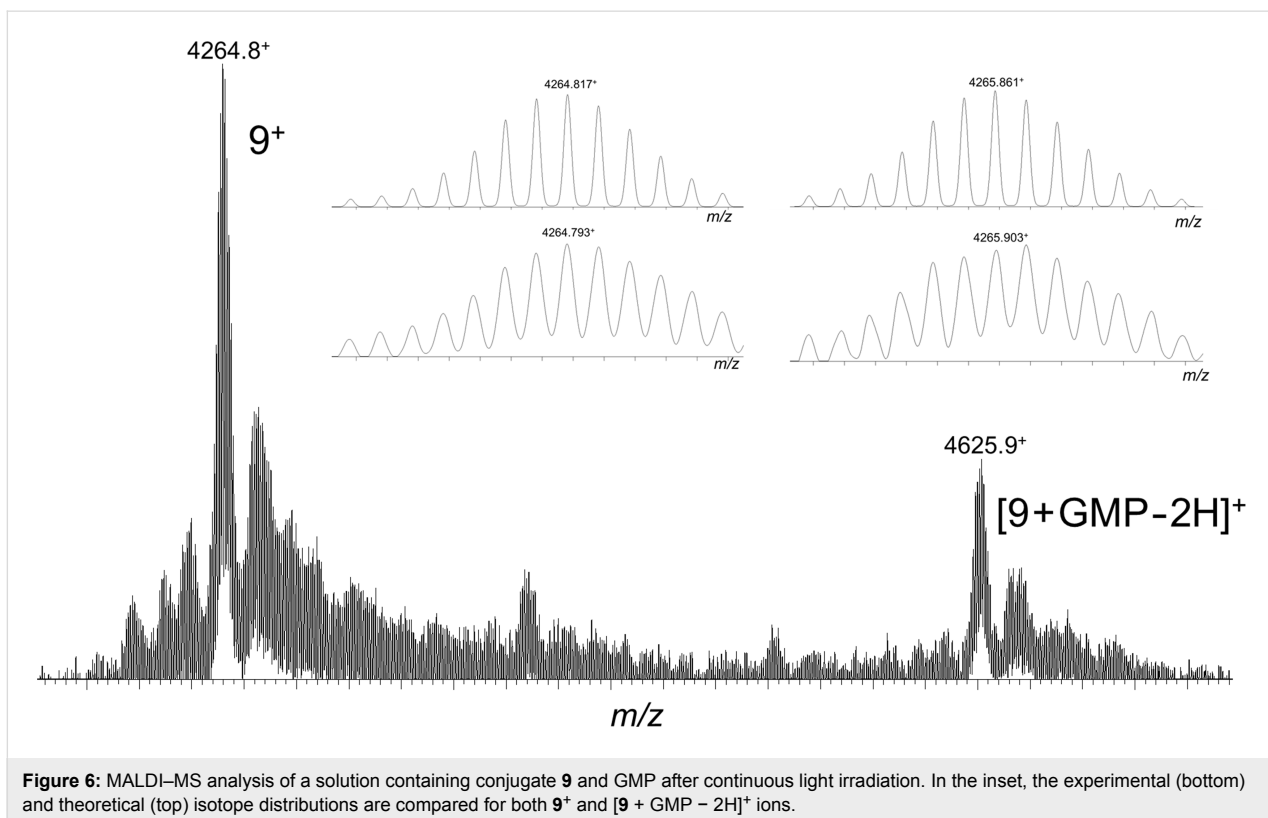


be observed around 500 nm on a long time scale. This transient is specific of a monoreduced Ru^{II}-TAP^{•-} species [81], confirming that a PET occurs.

To verify if a photoadduct can be obtained between the complex anchored on the calixarene platform and a guanine base, a continuous irradiation of a solution containing conjugate **9** and GMP was achieved. The crude irradiation mixture was then analyzed by MALDI mass spectrometry (HRMS, Figure 6). Alongside the parent conjugate **9** ions, ionized species at higher mass-to-charge ratio ($m/z = 4625.9$) are detected and formally correspond to the addition of GMP minus two hydrogen atoms. The comparison between the experimental and theoretical isotope patterns confirms (inset Figure 6) that irradiation of conjugate **9** and GMP efficiently yielded the desired photoadduct.

Conclusion

The present work validates the design strategy that consists in using calix[4]arenes as addressable platforms for the elaboration of multivalent photoreactive systems that could potentially target and enter cancer cells. The selective tethering of a photoreactive Ru-TAP complex on the small rim of a calix[4]arene and the introduction of four c-[RGDfK] moieties on its large rim were efficiently achieved. In good agreement with molecular modeling simulations, it was shown that the



photophysical properties of the tethered complex **9** are not altered by the anchoring onto the calixarene platform and that the cyclic pentapeptide units do not interfere with the photoreactivity of the complex. Moreover, we verified that the complex is able to photoreact with its biological target, i.e., the guanine content of DNA, by demonstrating the occurrence of a photoinduced electron transfer and the formation of a covalent photoadduct between the Ru-calix(RGD)₄ conjugate **9** and GMP. In conclusion, the ruthenium complex should be able to perform efficiently its photoinduced cytotoxic activity, once incorporated into targeted cancer cells thanks to the multivalent platform. In cellulo studies are currently under investigation and will be reported in the near future.

Experimental

General: All the solvents and reagents for the syntheses were at least reagent grade quality and were used without further purification. Anhydrous *N,N*-dimethylformamide was purchased from ACROS Organics. Reactions were magnetically stirred and monitored by thin-layer chromatography using Fluka silica gel or aluminium oxide on TLC-PET foils with fluorescent indicator at 254 nm. All reactions involving ruthenium(II) were carried out in the dark. C18 reversed-phase silica gel (230–400 mesh) was used for chromatography. ¹H NMR spectra were recorded at ambient temperature on Bruker 300, Variant 400 and 600 MHz spectrometers and ¹³C NMR spectra were recorded at 75, 100 or 150 MHz. Traces of residual solvents were used as internal standards for ¹H NMR (7.26 ppm for CDCl₃, 3.31 for CD₃OD, 4.79 for D₂O, 2.50 for DMSO-*d*₆ and 1.94 ppm for CD₃CN) and ¹³C NMR (77.16 ppm for CDCl₃, 49.00 for CD₃OD, 39.52 for DMSO-*d*₆ and 118.26 ppm for CD₃CN) chemical shift referencing. Abbreviations: s = singlet, d = doublet, t = triplet, q = quartet, br = broad, m = massif, mult = multiplet). 2D NMR spectra (COSY, HSQC, HMBC, HSQC) were recorded to complete signal assignments. Melting points were recorded on a Stuart Scientific Analogue SMP11 or Büchi Melting Point B-545. Infrared spectra were recorded on a Bruker Alpha (ATR) spectrometer.

High-resolution mass spectra were obtained on a Waters Synapt G2-Si spectrometer (Waters, Manchester, UK) equipped with an electrospray ionization used in the positive ion mode. Source parameters were as follow: capillary voltage, 3.1 kV; sampling cone, 30 V; source Offset, 80 V; source temperature, 150 °C and desolvation temperature, 200 °C. Matrix-assisted laser desorption/ionization time-of-flight (MALDI-ToF) mass spectra were recorded using a Waters QToF Premier mass spectrometer equipped with a Nd-YAG laser of 355 nm with a maximum pulse energy of 65 μJ delivered to the sample at 50 Hz repeating rate. Time-of-flight mass analyses were performed in the reflection mode at a resolution of about 10 000. The matrix, *trans*-2-

(3-(4-*tert*-butylphenyl)-2-methyl-2-propenylidene)malononitrile, was prepared as a 40 mg/mL solution in chloroform. The matrix solution (1 μL) was applied to a stainless-steel target and air-dried. The crude photoirradiation product was dissolved in acetonitrile and 1 μL aliquot of this solution was applied onto the target area (already bearing the matrix crystals) and then air-dried.

The HPLC purification process on final compound **9** was performed on a semi-preparative Infinity Agilent 1290 UHPLC system equipped with a binary pump, a thermostatically controlled injection system, a thermostatically controlled column compartment and a Diode Array detector. Waters C18 (Atlantis T3) column was used and the elution conditions are described in Supporting Information File 1.

Calix[4]arenes **2** and **3** were synthesized from commercial *p*-*tert*-butylcalix[4]arene **1** according to procedures described in the literature [69]. The experimental procedures and characterization data for calixarene derivatives **4**, **6**, **7** and **9**, phenanthroline derivative **5** and *c*-[RGDfK]-alkyne **8** are given in Supporting Information File 1.

The UV–vis absorption spectra were recorded on a Perkin-Elmer Lambda UV–vis spectrophotometer and the emission spectra with a Shimadzu RF-5001 PC spectrometer (detection: Hamamatsu R-928 red-sensitive photomultiplier tube, excitation source: xenon lamp 250 W). Emission quantum yields were determined by integrating the corrected emission spectra over the frequencies. [Ru(bpy)₃]²⁺ in water under air was chosen as the standard luminophore (quantum yield of 0.042 under argon). The luminescence lifetimes were measured by the time-correlated single photon counting (TC-SPC) technique with the Edinburgh Instruments LifeSpecII Picosecond Fluorescence Lifetime Spectrometer equipped with a laser diode (λ = 439 nm, pulse = 100 ps). The samples were thermostatted at 20 ± 2 °C with a Haake Model NB22 temperature controller. The data were collected by a multichannel analyzer (2048 channels) with a number of counts in the first channel equal to 104. The resulting decays were deconvoluted for the instrumental response and fitted to the exponential functions using the original manufacturer software package (Edinburgh Instruments). The reduced χ², weighted residuals and autocorrelation function were employed to judge the quality of the fits.

For molecular modelling simulations, the initial structure of the ruthenium complex was obtained from previous DFT calculations using a previously reported methodology [82]. The geometries of the RAFTs and calixarene were built using DS BIOVIA[®] software and geometry-optimized using the CHARMM force-field, taking into account previous molecular

modelling simulations on cyclic peptides [83]. The structures were linked together yielding through several steps of energy minimizations, maintaining the ruthenium complex constrained in octahedral geometry by harmonic constraints. After energy minimization of the entire structure, MD simulations of 5 ns were produced in NVT ensemble at 300 K, in the generalized Born implicit solvent model. Although the MD simulation time used here is way insufficient to probe the conformational landscape of this large molecule, the conformations reported here represent relaxed geometries showing possible intermolecular contacts between the cyclic pentapeptides. The analysis and visualization of MD simulations were carried out using DS BIOVIA and Chimera [84] software.

Supporting Information

Supporting Information File 1

Supplementary information.

[<https://www.beilstein-journals.org/bjoc/content/supplementary/1860-5397-14-150-S1.pdf>]

Acknowledgements

S.K. thanks the Fonds pour la Formation à la Recherche dans l'Industrie et dans l'Agriculture (FRIA-FRS, Belgium) for her PhD grant. C.M. and M.S. thank the F.R.S.-FNRS ("Fonds National pour la Recherche Scientifique", Belgium) for continuing support, notably through the grants 2.4530.12, 2.4615.11, UN02715F, CDR J.0022.18, and F.4532.16. This work was also supported by the COST action CM 1202 and a "10 km de Bruxelles" grant. The mass spectrometry laboratory @ UMONS is grateful to the "Fonds National pour la Recherche Scientifique" (FNRS-Belgium) for financial support in the acquisition of the Waters QTOF premier and the Waters Synapt G2-Si mass spectrometers. D.B. and E.D. acknowledge support from the French National Research Agency (Labex program ARCANÉ, ANR-11-LABX-0003-01). L.M. thanks Pr. Kristin Bartik and Pr. Benjamin Elias for their continuing support. I.J. thanks the "Actions de Recherches Concertées" of the Fédération Wallonie-Bruxelles and the ULB for financial support.

ORCID® iDs

Sofia Kajouj - <https://orcid.org/0000-0002-6105-1691>

Lionel Marcelis - <https://orcid.org/0000-0002-6324-477X>

Pierre Van Antwerpen - <https://orcid.org/0000-0002-4934-8863>

Didier Boturyn - <https://orcid.org/0000-0003-2530-0299>

Eric Defrancq - <https://orcid.org/0000-0002-3911-6241>

Mathieu Surin - <https://orcid.org/0000-0001-8950-3437>

Julien De Winter - <https://orcid.org/0000-0003-3429-5911>

Pascal Gerbaux - <https://orcid.org/0000-0001-5114-4352>

Ivan Jabin - <https://orcid.org/0000-0003-2493-2497>

Cécile Moucheron - <https://orcid.org/0000-0001-9293-0165>

References

- Kirch, M.; Lehn, J. M.; Sauvage, J.-P. *Helv. Chim. Acta* **1979**, *62*, 1345–1384. doi:10.1002/hlca.19790620449
- Juris, A.; Balzani, V.; Barigelletti, F.; Campagna, S.; Belser, P.; von Zelewsky, A. *Coord. Chem. Rev.* **1988**, *84*, 85–277. doi:10.1016/0010-8545(88)80032-8
- Dare-Edwards, M. P.; Goodenough, J. B.; Hamnett, A.; Seddon, K. R.; Wright, R. D. *Faraday Discuss. Chem. Soc.* **1980**, *70*, 285–298. doi:10.1039/dc9807000285
- Puntoriero, F.; Sartorel, A.; Orlandi, M.; La Ganga, G.; Serroni, S.; Bonchio, M.; Scandola, F.; Campagna, S. *Coord. Chem. Rev.* **2011**, *255*, 2594–2601. doi:10.1016/j.ccr.2011.01.026
- Friedman, A. E.; Chambron, J. C.; Sauvage, J. P.; Turro, N. J.; Barton, J. K. *J. Am. Chem. Soc.* **1990**, *112*, 4960–4962. doi:10.1021/ja00168a052
- Boynton, A. N.; Marcélis, L.; Barton, J. K. *J. Am. Chem. Soc.* **2016**, *138*, 5020–5023. doi:10.1021/jacs.6b02022
- Deraedt, Q.; Marcélis, L.; Auvray, T.; Hanan, G. S.; Loiseau, F.; Elias, B. *Eur. J. Inorg. Chem.* **2016**, *2016*, 3649–3658. doi:10.1002/ejic.201600468
- Deraedt, Q.; Marcélis, L.; Loiseau, F.; Elias, B. *Inorg. Chem. Front.* **2017**, *4*, 91–103. doi:10.1039/C6QI00223D
- Boynton, A. N.; Marcélis, L.; McConnell, A. J.; Barton, J. K. *Inorg. Chem.* **2017**, *56*, 8381–8389. doi:10.1021/acs.inorgchem.7b01037
- Piroux, G.; Bar, L.; Abraham, M.; Lavergne, T.; Jamet, H.; Dejeu, J.; Marcélis, L.; Defrancq, E.; Elias, B. *Chem. – Eur. J.* **2017**, *23*, 11872–11880. doi:10.1002/chem.201702076
- Saadallah, D.; Bellakhal, M.; Amor, S.; Lefebvre, J.-F.; Chavarot-Kerlidou, M.; Baussanne, I.; Moucheron, C.; Demeunynck, M.; Monchaud, D. *Chem. – Eur. J.* **2017**, *23*, 4967–4972. doi:10.1002/chem.201605948
- Feeney, M. M.; Kelly, J. M.; Tossi, A. B.; Kirsch-De Mesmaeker, A.; Lecomte, J.-P. *J. Photochem. Photobiol., B* **1994**, *23*, 69–78. doi:10.1016/1011-1344(93)06985-C
- Troian-Gautier, L.; Mugeniwabagara, E.; Fusaro, L.; Moucheron, C.; Kirsch-De Mesmaeker, A.; Luhmer, M. *Inorg. Chem.* **2016**, *56*, 1794–1803. doi:10.1021/acs.inorgchem.6b01780
- Troian-Gautier, L.; Mugeniwabagara, E.; Fusaro, L.; Cauët, E.; Kirsch-De Mesmaeker, A.; Luhmer, M. *J. Am. Chem. Soc.* **2017**, *139*, 14909–14912. doi:10.1021/jacs.7b09513
- Blasius, R.; Nierengarten, H.; Luhmer, M.; Constant, J.-F.; Defrancq, E.; Dumy, P.; van Dorsselaer, A.; Moucheron, C.; Kirsch-De Mesmaeker, A. *Chem. – Eur. J.* **2005**, *11*, 1507. doi:10.1002/chem.200400591
- Marcélis, L.; Ghesquière, J.; Garnir, K.; Kirsch-De Mesmaeker, A.; Moucheron, C. *Coord. Chem. Rev.* **2012**, *256*, 1569–1582. doi:10.1016/j.ccr.2012.02.012
- Ghesquière, J.; Le Gac, S.; Marcélis, L.; Moucheron, C.; Kirsch-De Mesmaeker, A. *Curr. Top. Med. Chem.* **2012**, *12*, 185–196. doi:10.2174/156802612799079008
- Garnir, K.; Estalayo-Adrián, S.; Lartia, R.; De Winter, J.; Defrancq, E.; Surin, M.; Lemaire, V.; Gerbaux, P.; Moucheron, C. *Faraday Discuss.* **2015**, *185*, 267–284. doi:10.1039/C5FD00059A
- Estalayo-Adrián, S.; Garnir, K.; Moucheron, C. *Chem. Commun.* **2018**, *54*, 322–337. doi:10.1039/C7CC06542F
- Jacquet, L.; Davies, R. J. H.; Kirsch-De Mesmaeker, A.; Kelly, J. M. *J. Am. Chem. Soc.* **1997**, *119*, 11763–11768. doi:10.1021/ja971163z

21. Jacquet, L.; Kelly, J. M.; Kirsch-De Mesmaeker, A. *J. Chem. Soc., Chem. Commun.* **1995**, 913–914. doi:10.1039/C39950000913
22. Marcéls, L.; Rebarz, M.; Lemaur, V.; Fron, E.; De Winter, J.; Moucheron, C.; Gerbaux, P.; Beljonne, D.; Sliwa, M.; Kirsch-De Mesmaeker, A. *J. Phys. Chem. B* **2015**, *119*, 4488–4500. doi:10.1021/acs.jpcc.5b00197
23. Pauly, M.; Kayser, I.; Schmitz, M.; Dicato, M.; Del Guerso, A.; Kolber, I.; Moucheron, C.; Kirsch-De Mesmaeker, A. *Chem. Commun.* **2002**, 1086–1087. doi:10.1039/b202905g
24. Lentzen, O.; Defrancq, E.; Constant, J. F.; Schumm, S.; García-Fresnadillo, D.; Moucheron, C.; Dumy, P.; Kirsch-De Mesmaeker, A. *J. Biol. Inorg. Chem.* **2004**, *9*, 100–108. doi:10.1007/s00775-003-0502-3
25. Marcéls, L.; Moucheron, C.; Kirsch-De Mesmaeker, A. *Philos. Trans. R. Soc., A* **2013**, 371. doi:10.1098/rsta.2012.0131
26. Marcéls, L.; Surin, M.; Lartia, R.; Moucheron, C.; Defrancq, E.; Kirsch-De Mesmaeker, A. *Eur. J. Inorg. Chem.* **2014**, *2014*, 3016–3022. doi:10.1002/ejic.201402189
27. Reschner, A.; Bontems, S.; Le Gac, S.; Lambermont, J.; Marcéls, L.; Defrancq, E.; Hubert, P.; Moucheron, C.; Kirsch-De Mesmaeker, A.; Raes, M.; Piette, J.; Delvenne, P. *Gene Ther.* **2013**, *20*, 435–443. doi:10.1038/gt.2012.54
28. Marcéls, L.; Van Overstraeten-Schlögel, N.; Lambermont, J.; Bontems, S.; Spinelli, N.; Defrancq, E.; Moucheron, C.; Kirsch-De Mesmaeker, A.; Raes, M. *ChemPlusChem* **2014**, *79*, 1597–1604. doi:10.1002/cplu.201402212
29. Puckett, C. A.; Barton, J. K. *Biochemistry* **2008**, *47*, 11711–11716. doi:10.1021/bi800856t
30. Puckett, C. A.; Barton, J. K. *J. Am. Chem. Soc.* **2007**, *129*, 46–47. doi:10.1021/ja0677564
31. Matson, M.; Svensson, F. R.; Nordén, B.; Lincoln, P. *J. Phys. Chem. B* **2011**, *115*, 1706–1711. doi:10.1021/jp109530f
32. Svensson, F. R.; Matson, M.; Li, M.; Lincoln, P. *Biophys. Chem.* **2010**, *149*, 102–106. doi:10.1016/j.bpc.2010.04.006
33. Cloonan, S. M.; Elmes, R. B. P.; Erby, M. L.; Bright, S. A.; Poynton, F. E.; Nolan, D. E.; Quinn, S. J.; Gunnlaugsson, T.; Williams, D. C. *J. Med. Chem.* **2015**, *58*, 4494–4505. doi:10.1021/acs.jmedchem.5b00451
34. Byrne, A.; Dolan, C.; Moriarty, R. D.; Martin, A.; Neugebauer, U.; Forster, R. J.; Davies, A.; Volkov, Y.; Keyes, T. E. *Dalton Trans.* **2015**, *44*, 14323–14332. doi:10.1039/C5DT01833A
35. van Rijt, S. H.; Kosthunova, H.; Brabec, V.; Sadler, P. J. *Bioconjugate Chem.* **2011**, *22*, 218–226. doi:10.1021/bc100369p
36. Gamba, I.; Salvadó, I.; Rama, G.; Bertazzon, M.; Sánchez, M. I.; Sánchez-Pedregal, V. M.; Martínez-Costas, G.; Brissos, R. F.; Gamez, P.; Mascarenãs, J. L.; Vásquez-López, M.; Vásquez, M. E. *Chem. – Eur. J.* **2013**, *19*, 13369–13375. doi:10.1002/chem.201301629
37. Burke, C. S.; Byrne, A.; Keyes, T. E. *J. Am. Chem. Soc.* **2018**, *140*, 6945–6955. doi:10.1021/jacs.8b02711
38. Marcéls, L.; Kajouji, K.; Ghesquière, J.; Fettweis, G.; Coupienne, I.; Lartia, R.; Surin, M.; Defrancq, E.; Piette, J.; Moucheron, C.; Kirsch-De Mesmaeker, A. *Eur. J. Inorg. Chem.* **2016**, *2016*, 2902–2911. doi:10.1002/ejic.201600278
39. Max, R.; Gerritsen, R. R. C. M.; Nooijen, P. T. G. A.; Goodman, S. L.; Sutter, A.; Keilholz, U.; Ruiter, D. J.; De Waal, R. M. W. *Int. J. Cancer* **1997**, *71*, 320–324. doi:10.1002/(SICI)1097-0215(19970502)71:3<320::AID-IJC2>3.0.CO;2-#
40. Ferrara, N.; Kerbel, R. S. *Nature* **2005**, *438*, 967–974. doi:10.1038/nature04483
41. Haubner, R.; Gratiyas, R.; Diefenbach, B.; Goodman, S. L.; Jonczyk, A.; Kessler, H. *J. Am. Chem. Soc.* **1996**, *118*, 7461–7472. doi:10.1021/ja9603721
42. Dechantsreiter, M. A.; Planker, E.; Mathä, B.; Lohof, E.; Hölzemann, G.; Jonczyk, A.; Goodman, S. L.; Kessler, H. *J. Med. Chem.* **1999**, *42*, 3033–3040. doi:10.1021/jm970832g
43. Castel, S.; Pagan, R.; Mitjans, F.; Piulats, J.; Goodman, S.; Jonczyk, A.; Huber, F.; Vilaró, S.; Reina, M. *Lab. Invest.* **2001**, *81*, 1615–1626. doi:10.1038/labinvest.3780375
44. Mammen, M.; Choi, S.-K.; Whitesides, G. M. *Angew. Chem., Int. Ed.* **1998**, *37*, 2754–2794. doi:10.1002/(SICI)1521-3773(19981102)37:20<2754::AID-ANIE2754>3.CO;2-3
45. Kiessling, L. L.; Lamanna, A. C. Multivalency In Biological Systems. In *Chemical Probes in Biology*; Schneider, M. P., Ed.; Springer: Netherlands, 2003; Vol. 129, pp 345–357. doi:10.1007/978-94-007-0958-4_26
46. Gestwicki, J. E.; Cairo, C. W.; Strong, L. E.; Oetjen, K. A.; Kiessling, L. L. *J. Am. Chem. Soc.* **2002**, *124*, 14922–14933. doi:10.1021/ja027184x
47. Wu, Y.; Zhang, X.; Xiong, Z.; Cheng, Z.; Fisher, D. R.; Liu, S.; Gambhir, S. S.; Chen, X. *J. Nucl. Med.* **2005**, *46*, 1707–1718.
48. Ye, Y.; Bloch, S.; Xu, B.; Achilefu, S. *J. Med. Chem.* **2006**, *49*, 2268–2275. doi:10.1021/jm050947h
49. Shi, J.; Kim, Y.-S.; Zhai, S.; Liu, Z.; Chen, X.; Liu, S. *Bioconjugate Chem.* **2009**, *20*, 750–759. doi:10.1021/bc800455p
50. Wenk, C. H. F.; Ponce, F.; Guillermet, S.; Tenaud, C.; Boturyn, D.; Dumy, P.; Watrelot-Virieux, D.; Carozzo, C.; Josserand, V.; Coll, J.-L. *Cancer Lett.* **2013**, *334*, 188–195. doi:10.1016/j.canlet.2012.10.041
51. Temming, K.; Meyer, D. L.; Zabinski, R.; Dijkers, E. C. F.; Poelstra, K.; Molema, G.; Kok, R. *J. Bioconjugate Chem.* **2006**, *17*, 1385–1394. doi:10.1021/bc060087z
52. Foillard, S.; Sancey, L.; Coll, J.-L.; Boturyn, D.; Dumy, P. *Org. Biomol. Chem.* **2009**, *7*, 221–224. doi:10.1039/B817251J
53. Karageorgis, A.; Claron, M.; Jugé, R.; Aspord, C.; Leloup, C.; Thoreau, F.; Kurchaczak, J.; Plumas, J.; Henry, M.; Hurbin, A.; Verdié, P.; Martinez, J.; Subra, G.; Dumy, P.; Boturyn, D.; Auouacheria, A.; Coll, J.-L. *Mol. Ther.* **2017**, *25*, 534–546. doi:10.1016/j.ymthe.2016.11.002
54. Gutsche, C. D. Calixarenes: An introduction. 2nd ed.; Stoddart, J. F., Ed.; Monographs in Supramolecular Chemistry; The Royal Society of Chemistry: Cambridge, 2008. doi:10.1039/9781847558190
55. Lavendomme, R.; Zahim, S.; De Leener, G.; Inthasot, A.; Mattiuzzi, A.; Luhmer, M.; Reinaud, O.; Jabin, I. *Asian J. Org. Chem.* **2015**, *4*, 710–722. doi:10.1002/ajoc.201500178
56. Mattiuzzi, A.; Il; Marcéls, L.; Jabin, I.; Moucheron, C.; Kirsch-De Mesmaeker, A. *Inorg. Chem.* **2013**, *52*, 11228–11236. doi:10.1021/ic401468t
57. Casnati, A.; Sansone, F.; Ungaro, R. *Acc. Chem. Res.* **2003**, *36*, 246–254. doi:10.1021/ar0200798
58. Giuliani, M.; Morbioli, I.; Sansone, F.; Casnati, A. *Chem. Commun.* **2015**, *51*, 14140–14159. doi:10.1039/C5CC05204A
59. Sansone, F.; Casnati, A. *Chem. Soc. Rev.* **2013**, *42*, 4623–4639. doi:10.1039/c2cs35437c
60. Sun, J.; Blaskovich, M. A.; Jain, R. K.; Delarue, F.; Paris, D.; Brem, S.; Wotoczek-Obadia, M.; Lin, Q.; Coppola, D.; Choi, K.; Mullan, M.; Hamilton, A. D.; Sebt, S. M. *Cancer Res.* **2004**, *64*, 3586–3592. doi:10.1158/0008-5472.CAN-03-2673

61. Baldini, L.; Casnati, A.; Sansone, F.; Ungaro, R. *Chem. Soc. Rev.* **2007**, *36*, 254–266. doi:10.1039/B603082N
62. Sansone, F.; Baldini, L.; Casnati, A.; Ungaro, R. *New J. Chem.* **2010**, *34*, 2715–2728. doi:10.1039/c0nj00285b
63. Le Poul, N.; Le Mest, Y.; Jabin, I.; Reinaud, O. *Acc. Chem. Res.* **2015**, *48*, 2097–2106. doi:10.1021/acs.accounts.5b00152
64. Nimse, S. B.; Kim, T. *Chem. Soc. Rev.* **2013**, *42*, 366–386. doi:10.1039/C2CS35233H
65. Haubner, R.; Wester, H.-J.; Burkhart, F.; Senekowitsch-Schmidtke, R.; Weber, W.; Goodman, S. L.; Kessler, H.; Schwaiger, M. *J. Nucl. Med.* **2001**, *42*, 326–336.
66. Dondoni, A.; Marra, A. *Chem. Rev.* **2010**, *110*, 4949–4977. doi:10.1021/cr100027b
67. Rostovtsev, V. V.; Green, L. G.; Fokin, V. V.; Sharpless, K. B. *Angew. Chem., Int. Ed.* **2002**, *41*, 2596–2599. doi:10.1002/1521-3773(20020715)41:14<2596::AID-ANIE2596>3.0.CO;2-4
68. Meldal, M.; Tornøe, C. W. *Chem. Rev.* **2008**, *108*, 2952–3015. doi:10.1021/cr0783479
69. Mattiuzzi, A.; Jabin, I.; Mangeney, C.; Roux, C.; Reinaud, O.; Santos, L.; Bergamini, J.-F.; Hapiot, P.; Lagrost, C. *Nat. Commun.* **2012**, *3*, No. 1130. doi:10.1038/ncomms2121
70. Ikeda, A.; Shinkai, S. *Chem. Rev.* **1997**, *97*, 1713–1734. doi:10.1021/cr960385x
71. Deroo, S.; Defrancq, E.; Moucheron, C.; Kirsch-De Mesmaeker, A.; Dumy, P. *Tetrahedron Lett.* **2003**, *44*, 8379–8382. doi:10.1016/j.tetlet.2003.09.128
72. Kolb, H. C.; Sharpless, K. B. *Drug Discovery Today* **2003**, *8*, 1128–1137. doi:10.1016/S1359-6446(03)02933-7
73. Consoli, G. M. L.; Granata, G.; Fragassi, G.; Grossi, M.; Sallese, M.; Geraci, C. *Org. Biomol. Chem.* **2015**, *13*, 3298–3307. doi:10.1039/C4OB02333A
74. Bew, S. P.; Brimage, R. A.; L'Hermite, N.; Sharma, S. V. *Org. Lett.* **2007**, *9*, 3713–3716. doi:10.1021/ol071047t
75. Ryu, E.-H.; Zhao, Y. *Org. Lett.* **2005**, *7*, 1035–1037. doi:10.1021/ol047468h
76. Rusu, R.; Szumna, A.; Rosu, N.; Dumea, C.; Danac, R. *Tetrahedron* **2015**, *71*, 2922–2926. doi:10.1016/j.tet.2015.03.060
77. Vecchi, A.; Melai, B.; Marra, A.; Chiappe, C.; Dondoni, A. *J. Org. Chem.* **2008**, *73*, 6437–6440. doi:10.1021/jo800954z
78. Zahim, S.; Lavendomme, R.; Reinaud, O.; Luhmer, M.; Evano, G.; Jabin, I. *Org. Biomol. Chem.* **2016**, *14*, 1950–1957. doi:10.1039/C5OB02367J
79. Gawande, M. B.; Goswami, A.; Felpin, F.-X.; Asefa, T.; Huang, X.; Silva, R.; Zou, X.; Zboril, R.; Varma, R. S. *Chem. Rev.* **2016**, *116*, 3722–3811. doi:10.1021/acs.chemrev.5b00482
80. No such aggregates were detected when the conjugate **9** was used in Tris-HCl buffer for photochemical experiments.
81. Rebarz, M.; Marcélis, L.; Menand, M.; Cornut, D.; Moucheron, C.; Jabin, I.; Kirsch-De Mesmaeker, A. *Inorg. Chem.* **2014**, *53*, 2635–2644. doi:10.1021/ic403024z
82. Ghizdavu, L.; Pierard, F.; Rickling, S.; Aury, S.; Surin, M.; Beljonne, D.; Lazzaroni, R.; Murat, P.; Defrancq, E.; Moucheron, C.; Kirsch-De Mesmaeker, A. *Inorg. Chem.* **2009**, *48*, 10988–10994. doi:10.1021/ic901007w
83. Marinelli, L.; Lavecchia, A.; Gottschalk, K.-E.; Novellino, E.; Kessler, H. *J. Med. Chem.* **2003**, *46*, 4393–4404. doi:10.1021/jm020577m
84. Pettersen, E. F.; Goddard, T. D.; Huang, C. C.; Couch, G. S.; Greenblatt, D. M.; Meng, E. C.; Ferrin, T. E. *J. Comput. Chem.* **2004**, *25*, 1605–1612. doi:10.1002/jcc.20084

License and Terms

This is an Open Access article under the terms of the Creative Commons Attribution License (<http://creativecommons.org/licenses/by/4.0>). Please note that the reuse, redistribution and reproduction in particular requires that the authors and source are credited.

The license is subject to the *Beilstein Journal of Organic Chemistry* terms and conditions:

(<http://www.beilstein-journals.org/bjoc>)

The definitive version of this article is the electronic one which can be found at:

doi:10.3762/bjoc.14.150